Student Projects

Elaboration on the Hexagonal Grid and Spiral Method for Data Collection Via Pole Figures

Anthony C. Rizzie

Anthony Rizzie is a junior majoring in Mathematics (Opt. 1) with a double minor in Physics and Spanish. He plans to graduate in May 2009 and pursue a Ph.D. in Math. He interned at Oak Ridge National Laboratory under the supervision of Dr. Thomas R. Watkins and Dr. E. Andrew Payzant in the summer of 2007, where they conducted the research for this article.

There exist various techniques to "scan" an object using x-rays, the most common of which uses a polar sampling grid, all relying on the diffraction equation known as Bragg's Law [1, 6]. During my internship at Oak Ridge National Laboratory, I investigated the uses and efficiency of application of two specific types of grids: a hexagonal grid and a spiral grid, details of which are given below. The hexagonal [2, 3, 4] and spiral [5] methods have been introduced and used previously, without including the mathematical details necessary to actually implement these methods. I developed the algorithms necessary to generate each grid and implemented them (by writing computer code) to test my results.

Overview

Pole figures provide a graphical representation of the orientation of objects in space. They represent the distribution of a particular set of atomic planes for data acquired through diffraction and are used for analyzing crystallographic texture in materials science.

A four-circle goniometer is usually employed to collect pole figures. Here, the detector (θ-axis) is set at the Bragg angle (the angle between an incident x-

ray beam and a set of crystal planes for which the secondary radiation displays maximum intensity as a result of constructive interference) and the sample (ω-axis) is often set at half the Bragg angle.

The desired reflection intensity is measured over a set of sample tilt angles (χ) and azimuthal angles (ϕ) (see Figure 1). Typically, this data is presented in a pole figure. The Schulz method collects pole figure data using a $5^\circ \times 5^\circ$ ($\chi \times \phi$) grid (see Figure 2). Pole figure data can be viewed in a variety of ways, including stereographic and equal area projections on a plane. The main difference between the two is that stereographic projections preserve angle measurements but not area proportions, while equal area projections preserve area proportions but not angle measure [4]. The spiral grid is a stereographic projection of the hemisphere, while the hexagonal grid is an equal area projection. The type of projection to be used depends on whether the goal is to preserve angle measurements or keep surface areas proportional when projecting from the hemisphere. While data can be displayed using either type of projection, the nature of the grid points may not be preserved. Displayed in stereographic projection, the hexagonal grid will not feature the same layout and equal spacing between data points. Similarly, the spiral grid would be distorted in an equal area projection since the spiral's angular nature is no longer preserved (comparisons with actual data can be seen in Figure 7).

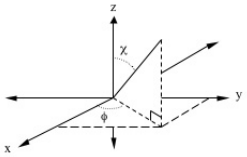

Figure 1: Three-dimensional representation of the measurement angles χ and ϕ. The z-axis is normal to the initial mounting surface of the sample.

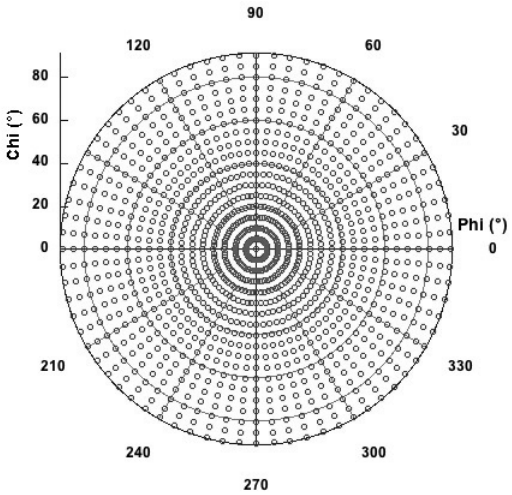

Figure 2: $5^\circ\chi \times 5^\circ\phi$ grid used in the Schulz method [polar plot].

The Hexagonal Grid

The hexagonal grid data collection method removes the over- and under-sampling at low and high χ values, respectively, using the Schulz method [4]; the density of sample points (as shown in Figure 2) is greater near the origin. The first step of the hexagonal grid method is to determine the number of desired data points. This is done by selecting R, the maximum desired χ value and N, the number of equal line segments along the central/east radius (see Figure 3). Next, using a grid made up of rows of equilateral triangles (see Figure 4), a hexagonal grid in Cartesian (x, y) coordinates can be constructed using equations (1)–(5) below.

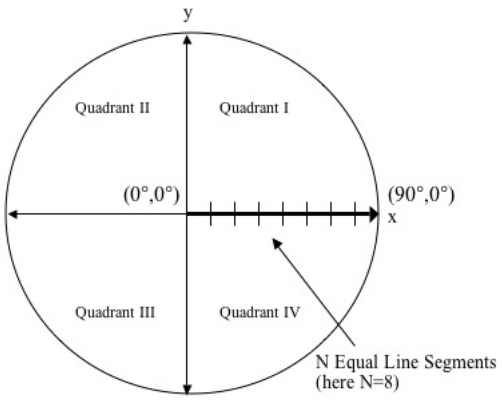

Figure 3: Determination of the constant N.

First and second quadrants:

$$|y_j| \leq R \tag{1}$$

$$y_j = \frac{\sqrt{3}R}{2N} j, \ j = 0, 1, 2, \ldots \tag{2}$$

$$|x_{ij}| \leq \sqrt{R^2 - (y_j)^2} \tag{3}$$

$$x_{ij} = \begin{cases} \dfrac{R}{N} i, & \text{if } j \equiv 0 \bmod 2 \quad (4) \\ \dfrac{R}{2N} + \dfrac{R}{N} i, & \text{if } j \equiv 1 \bmod 2 \quad (5) \end{cases}$$

$$\chi_{ij} = \sqrt{(x_{ij})^2 + (y_j)^2} \tag{6}$$

$$\phi_{ij} = \begin{cases} \left(\frac{180^\circ}{\pi}\right) \arctan\left(\frac{y_j}{x_{ij}}\right), & \text{if } x_{ij} > 0 \quad (7) \\ 90^\circ, & \text{if } x_{ij} = 0 \quad (8) \\ \left(\frac{180^\circ}{\pi}\right) \arctan\left(\frac{y_j}{x_{ij}}\right) + 180^\circ, & \text{if } x_{ij} < 0 \quad (9) \end{cases}$$

Third and fourth quadrants:

omit points where $y = 0$,

$$\chi_{ij} = \sqrt{(x_{ij})^2 + (y_j)^2} \quad (6)$$

$$\phi_{ij} = \begin{cases} \left(\frac{180^\circ}{\pi}\right) \arctan\left(\frac{y_j}{x_{ij}}\right) + 180^\circ, & \text{if } x_{ij} > 0 \quad (10) \\ 270^\circ, & \text{if } x_{ij} = 0 \quad (11) \\ \left(\frac{180^\circ}{\pi}\right) \arctan\left(\frac{y_j}{x_{ij}}\right) + 360^\circ, & \text{if } x_{ij} < 0 \quad (12) \end{cases}$$

The values of y_j are calculated using the increasing index values j (2), starting with $j = 0$ and corresponding $y_0 = 0$, until the last generated y_j is as close as possible to the radius R without exceeding it, still satisfying inequality (1). The y_j values also depend on the height of equilateral triangles with the side length $\frac{R}{N}$ (see Figure 4 below). All the corresponding x_{ij} values at each j are then calculated using (3)–(5) for specific i values. In Quadrants I and II, the x values start at either $x = 0$ (4) or $x = \frac{R}{2N}$ (5), and the spacing between each value is a multiple of $\frac{R}{N}$, which is calculated by using another index i. The x_{ij} values alternate between two distinct patterns, depending on whether j is even or odd. For each fixed value of y_j, the x_{ij} values can then be determined, up to the boundary of the circle with radius R (3). The values of χ and ϕ are then found by transforming each point (x, y) to polar coordinates, equations (6)–(9). Each value of χ_{ij} is equivalent to the length of the hypotenuse of the right triangle formed by x_{ij} and y_j (6). Each ϕ_{ij} is the arctangent of the ratio $\frac{y}{x}$, multiplied by $\frac{180^\circ}{\pi}$ to transform radians to degrees, (7)–(9). Since the arctangent function's range is $(-90^\circ, 90^\circ)$, the new points may not lie in the correct quadrant or, in some cases, may be undefined. In such case, a point can be rotated to the correct position by adding 0° for $x_{ij} > 0$, as in (7), or 180° for $x_{ij} < 0$, as in (9). When $x_{ij} = 0$ and $y_{ij} > 0$, ϕ must be defined as 90° (8) (to avoid division by 0). Due to the symmetry of the graph, points in Quadrants III and IV can be obtained by 180° rotations (10)–(12) of all the points in Quadrants I and II, which is equivalent to reflection. Points with $y_j = 0$, however, must be omitted so they are not duplicated or doubled.

The χ_{ij} values in Quadrants III and IV are the same due to symmetry (6). Figure 5 shows an example of a hexagonal grid.

Just as with the $5^\circ \times 5^\circ$ grid for the Schultz method, projecting the hexagonal grid points in the plane back onto the hemisphere gives us the set of angles to be scanned by the goniometer. Both methods collect data by scanning the different ϕ values for each specific χ, beginning at 0 and increasing up to the maximum value. In each case, the grid points lie in circles (one for each fixed χ), although for the hexagonal method, the number of points on each circle varies.

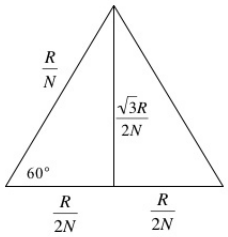

Figure 4: Dimensions of a triangle in the hexagonal grid.

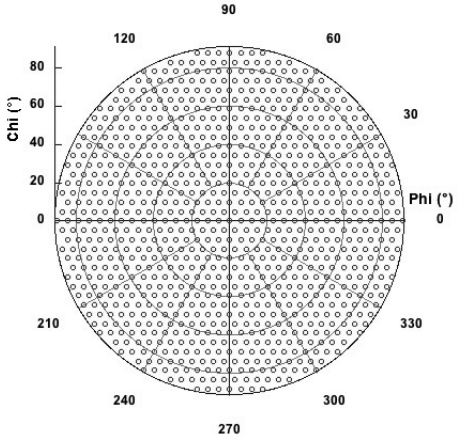

Figure 5: Hexagonal grid with $N = 16$ and $R = 90^\circ$ (Equal Area Projection).

The Spiral Method

The spiral is a path of constant angular direction on the hemisphere (like a ship traveling from a pole to the equator with a constant compass direction). The spiral lends itself well to an efficient means of collecting pole figure data because its radius increases quicker than the $5^\circ \times 5^\circ$ grid with fewer points overall. If equipment with such capabilities is available, the angles χ_n and ϕ_n can be continuously adjusted along the path of the spiral. Since this is

not always possible, discrete points of the spiral can be generated using the following equations:

$$\phi_n = \phi_{n-1} + \frac{5\chi_{\max}}{\chi_{n-1}} \tag{13}$$

$$\chi_n = \begin{cases} 5^\circ, \text{ if } \phi = 0^\circ & (14) \\ e^{b\phi_n}, \text{ if } 0^\circ < \phi < \phi_{\max} \text{ (omit if } \chi < 5^\circ) & (15) \\ \chi_{\max}, \text{ if } \phi = \phi_{\max} & (16) \end{cases}$$

where we must add $(0^\circ, 0^\circ)$ and where

$$b = \frac{\ln(\chi_{\max})}{\phi_{\max}} \tag{17}$$

The points of a spiral can be calculated using polar equations, making computation much less complicated. A spiral is an exponential curve in polar form, and most of the χ_n values are directly calculated by evaluating $e^{b\phi}$ (15), where n represents the term number of the recursively defined sequence (13) not exceeding $\phi_{\max}$. A logarithmic spiral is infinite in nature, and since $e^{b\phi}$ can never be 0, the point $(0^\circ, 0^\circ)$ must be defined separately. In order to avoid over-sampling at low χ values, all points with χ_n less than 5° should be omitted (15). The points $(5^\circ, 0^\circ)$ and $(\chi_{\max}, \phi_{\max})$ are added by (14) and (16) for consistent starting and ending positions that correspond to the $5^\circ \times 5^\circ$ grid. The constant b is determined by (17) so that the maximum value of ϕ_n allows the spiral to end very close to $\chi_{\max}$. In order to maintain an approximately equal distance between points on the spiral, the increment by which ϕ_n changes is a function of χ_n (13). At points with low χ values the spacing is about $\chi_{\max}$, and at points with high χ values near $\chi_{\max}$, the spacing is small (about 5° here, as determined with the inclusion of 5 in the numerator in (13)).

Like the hexagonal grid, the actual angles to be scanned by the goniometer have not yet been determined, since this spiral has been generated as a stereographic projection. Similarly, each χ value is first scaled down by a factor of $1/45^\circ$. This scales values between 0° and 90° to values in the range between 0 and 2, appropriate for radii in a stereographic projection. The χ values for the sphere are then determined by taking $2\arctan(\chi/2)$, with these newly scaled values. Beginning at $\chi = 0$ and increasing χ until the maximum is reached allows for an efficient scan of the spiral grid.

Experimental Comparison

A sample of 13 μm thick aluminum foil was mounted with rubber cement, and data was collected for pole figures using the Schulz, hexagonal grid, and spiral methods as described above. Data points for the hexagonal grid and spiral method were programmed into the equipment. The results can be seen below in Figure 6, represented graphically with Mathematica software. All three show the same features.

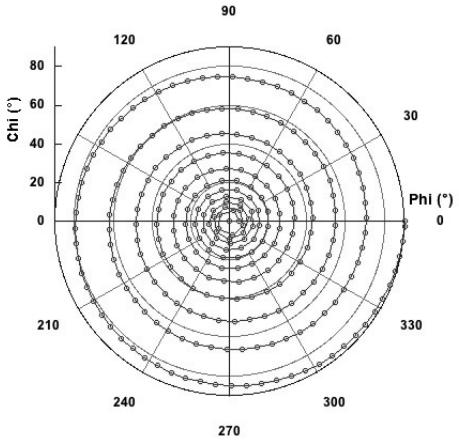

Figure 6: Spiral Grid with a maximum χ of 90° and a maximum ϕ of 6480° (Stereographic Projection).

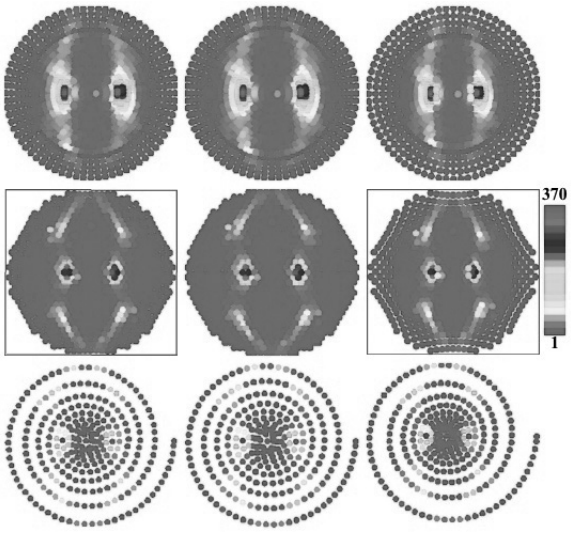

Figure 7: (111) Pole figures of aluminum foil: Schulz (top row), hexagonal grid (middle row), and spiral (bottom row) methods displayed as polar plots (left column), equal area (middle column) and stereographic projections (right column).

Summary

The mathematics for constructing and implementing the hexagonal grid and spiral method for pole figure data collection has been elaborated. Experimental measurements of aluminum foil resulted in typical rolling textures that compare favorably among the three methods [2]. The hexagonal grid eliminates the over-

and under-sampling of the Schulz method and uses approximately 40% less points with $N = 16$ and $R = 90°$. The spiral method has been shown to use over 75% less data points than the Schulz method but does not adequately collect a representative pole figure. In the future, implementation of the hexagonal grid and spiral method will be done using LabVIEW code.

Acknowledgments

The author would like to thank Dr. Lorch and Dr. Karls of Ball State University for their helpful discussion on Mathematica syntax and functions.

This research was sponsored by the Assistant Secretary for Energy Efficiency and Renewable Energy, Office of FreedomCAR and Vehicle Technologies, as part of the High Temperature Materials Laboratory User Program, Oak Ridge National Laboratory, managed by UT-Battelle, LLC, for the U.S. Department of Energy under contract number DE-AC05-00OR22725.

References

[1] B. Cullity and S. Stock, Elements of x-ray diffraction, Prentice Hall (2001).

[2] S. Matthies and H. Wenk, *Optimization of texture measurements by pole figure coverage with hexagonal grids*, Physica Status Solidi (A) **133** (2006) 253–257.

[3] L. Tarkowski, L. Laskosz and J. Bonarski, *Optimization of x-ray pole figure measurement*, Materials Science Forum **443/444** (2004) 137–140.

[4] U. Kocks, C. Tome and H. Wenk, Texture and anisotropy: Preferred orientation in polycrystals and their effect on materials properties, Cambridge University Press (1998).

[5] R. Eidelhorn, *Automatic Pole Figure Plotter*, The Review of Scientific Instruments **36** (1965) 997–1000.

[6] H. Krause and A. Haase, *X-ray diffraction system PTS for powder, texture and stress analysis*, pp. 405–408 in Experimental Techniques of Texture Analysis, DGM Informationsgesellschaft Verlag, Oberursel (1986) (H. Bunge, Editor).